

169 Crack Growth Mechanisms and Identification of Traction-Separation Relations in Antisymmetric CFRP Laminates

C. Blondeau¹, G. Pappas¹ and J. Botsis^{1a}

¹Laboratory of Applied Mechanics and Reliability Analysis (LMAF-STI),
Ecole Polytechnique Fédérale de Lausanne (EPFL), Lausanne CH-1015, Switzerland

^ajohn.botsis@epfl.ch

Introduction

Fibre composites (in particular carbon fibre reinforced polymers – CFRPs) are widely used in advanced applications because of their high specific strength and stiffness. However, their intrinsic laminated structure combined with the local mismatch of mechanical properties in mesoscale (due to different ply orientations) or constituents in microscale are responsible for their low toughness. Under applied mode I loading conditions, fracture of composites is accompanied of large scale bridging (LSB), greatly enhancing the resistance towards crack propagation. The phenomenon has been largely investigated on unidirectional (UD) laminates, using conventional double cantilever beam (DCB) specimen to quantify the evolution of the energy release rate (ERR). Numerous studies have also considered the fracture at interfaces between oriented plies, generally showing a stronger toughening effect than UD, due to LSB. However, the published results are not conclusive and illustrate the difficulties to isolate the effect of ply-angles on both toughening and fracture mechanisms. In particular, fracture of selected antisymmetric interfaces showed distinctive behaviour with phases of stable and unstable crack growths [1]. The aim of the present study was to investigate the influence of plies' orientation on the toughness and fracture morphology of antisymmetric interfaces [2].

Materials and Methods

Three types of antisymmetric interfaces ($+30^\circ/-30^\circ$, $+45^\circ/-45^\circ$ and $+60^\circ/-60^\circ$) were tested and compared to a UD reference, using DCB specimens submitted to mode I loading conditions. The different lay-ups were designed to reduce the distortion of the crack front (no skewness and minimal bowing) by minimizing the stiffness couplings [3, 4] and have comparable bending compliance of the individual DCB arms. The sequences were in the form of $[-\alpha/\alpha/-\alpha/R/+\alpha/-\alpha/+\alpha]_{\text{antisym}}$ (where $\alpha = 30^\circ, 45^\circ$ or 60° and R is a block of plies oriented at 0° or 90°). Specimens were manufactured using CFRP UD prepreg cured in an autoclave. The 60mm-long initial pre-crack was introduced by the insertion of a thin release film in-between the two central plies of the laminates. Prior to the test, the DCB specimens' sides were painted white, sprayed with speckles of black paint and graded every millimetre. The tests were conducted in displacement control at a rate of 3mm/min. For a selected specimen of $\pm 45^\circ$ series, the test was sequentially arrested at 3 crack advance levels. After each arrest the DCB was unloaded by 30% and submitted to X-ray micro-tomographic scanning (CT) to investigate the evolution of the crack morphology. To extract the resistance-curves, ERRs were computed from the expression of the J -integral $J = 2P \sin(\theta/2) / B$, as derived in [5], with P , the reaction load, θ , the crack mouth opening angle at the load application point and B , the width of the specimen. The traction-separation relations were obtained with the “direct method” by finite differentiation of ERRs with respect to crack opening displacements (CODs), δ . Three sets of side-views were acquired at a rate of 1Hz during the test to measure: (i) visually the crack advance, (ii) δ at the wake of the bridging zone by digital image correlation (DIC) using the a speckled pattern, and (iii) θ by DIC using two series of targets glued at the load application point.

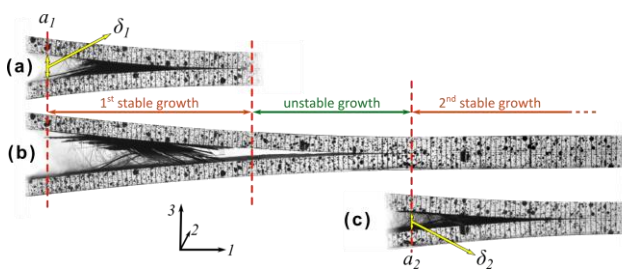


Fig. 1: Side-views (a) before the jump, (b) after the jump and (c) upon continued loading.

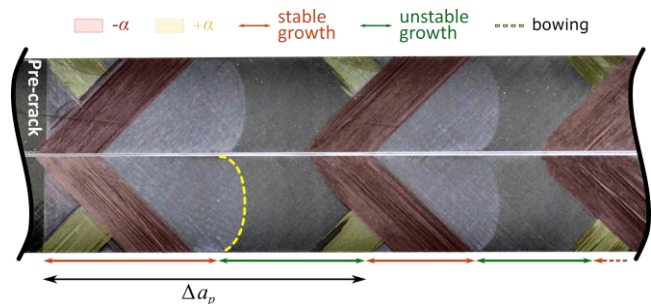


Fig. 2: Post-mortem conjugate fracture surfaces of a typical $\pm 45^\circ$ specimen.

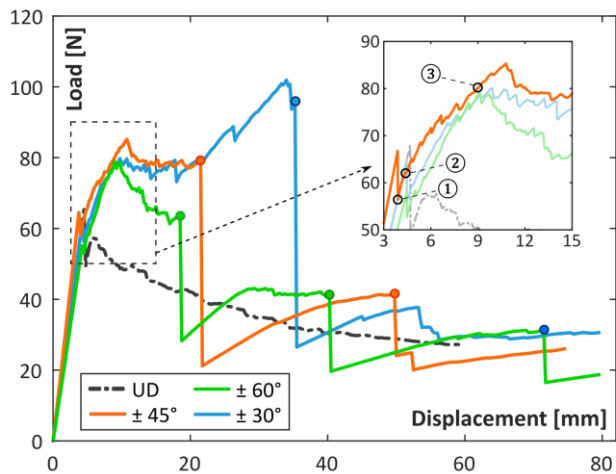


Fig. 3: Load-displacement curves of all tested interfaces (representative specimens and scatter, with dots indicating the start of jumps); insert shows loading levels at which CT-scans were performed [2].

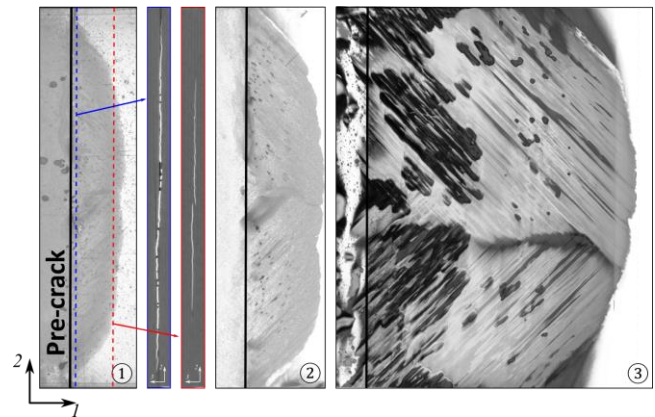


Fig. 4: Top-views of reconstructed CT-scans at the 3 levels of loading described in Fig. 3 (with cross-sections of the first scan), taken after 1h penetration of ZnI_2 based solution (voxel size of $14\mu m$).

Results and Discussion

All three types of antisymmetric interfaces showed a similar fracture response: at a_1 (see Fig. 1) crack initiation was followed by stable propagation related to intra-ply growth and formation of LSB. The first phase of stable propagation was followed by a sudden crack extension (herein, referred to as jump), corresponding to “pure” inter-ply growth and failure of the formed bridging (load drops in Fig. 3). At a_2 (see Fig. 1) stable growth restarted. The general process of stable/unstable propagation took place in a recurring manner, leading to the periodic fracture pattern observed in Fig. 2. As shown in Fig. 2, intra-ply propagation involved both adjacent plies, leading to a symmetric creation of bridging bands. As the bands overlapped in the middle of the specimen, new generation of bridging arrested and intra-ply propagation continued through a single ply, up to the jump where the crack migrated to the interlaminar region. The CT-scans in Fig. 4 demonstrate that the pop-in (point ①) corresponded to the creation of a bowed front, located mainly in the interlaminar region (with slight migration to intra-ply growth at the tip as shown by the cross-sections). Then upon further loading (point ②), the crack migrated towards the plies and intra-ply growth started leading to formation of LSB. The crack front was not affected by the loss of symmetry of the bridging pattern (from ③) and remained symmetric with constant bowing throughout the test as seen in Fig. 2: Post-mortem conjugate fracture surfaces of a typical $\pm 45^\circ$ specimen. Fig. 2 and Fig. 4 and also evidenced by the identical crack lengths and CODs, measured from each side of the specimen).

Experimental data showed that the ERR at initiation is practically independent of the interface angle, but the increase of the resistance was much lower for UD interfaces than the antisymmetric ones (for which it evolved inversely with the ply angle). The use of DIC for the measurement of CODs was well adapted to the recurring response of antisymmetric interfaces since the reference point could be reset after the jumps to capture the traction-separation relations along the different bridging regions (δ_1 and δ_2 in Fig. 4). For all antisymmetric series, the congruence of the J - δ data among the successive regions suggests that stable propagation was governed by a single relation. This hypothesis was confirmed by the implementation of the extracted traction-separation relations, due to bridging from the first loading phase, into finite element 2D cohesive models where the predicted numerical load-history matched well the experimental data for both the two first bridging zones (less than 4% mean relative error) [2].

References

- [1] W. Bradley, C. Corleto and D. Goetz, "Studies of mode I and mode II delamination using a J-integral analysis and in-situ observations of fracture in the SEM," 1990.
- [2] C. Blondeau, G. Pappas and J. Botsis, "Influence of ply-angle on fracture in antisymmetric interfaces of CFRP laminates," *Composite Structures*, vol. 216, pp. 464-476, 2019.
- [3] B. D. Davidson and R. A. Schapery, "Effect of Finite Width on Deflection and Energy Release rate of an Orthotropic Double Cantilever Specimen," *Journal of Composite Materials*, vol. 22, pp. 640-656, 1988.
- [4] B. D. Davidson, R. Krüger and M. König, "Effect of stacking sequence on energy release rate distributions in multidirectional DCB and ENF specimens," *Engineering Fracture Mechanics*, vol. 55, no. 4, pp. 557-569, 1996.
- [5] A. J. Paris and P. C. Paris, "Instantaneous evaluation of J and C^* ," *International Journal of Fracture*, vol. 38, pp. 19-21, 1988.

